



University of Dundee

Spectral matching and outdoor solar to electrical conversion efficiency in thin-film silicon multi-junction solar cells

Reynolds, S.; Urbain, F.; Smirnov, V.

Published in:
Journal of Physics: Conference Series

DOI:
[10.1088/1742-6596/794/1/012025](https://doi.org/10.1088/1742-6596/794/1/012025)

Publication date:
2017

Licence:
CC BY

Document Version
Publisher's PDF, also known as Version of record

[Link to publication in Discovery Research Portal](#)

Citation for published version (APA):
Reynolds, S., Urbain, F., & Smirnov, V. (2017). Spectral matching and outdoor solar to electrical conversion efficiency in thin-film silicon multi-junction solar cells. *Journal of Physics: Conference Series*, 794(1), 1-6. Article 012025. <https://doi.org/10.1088/1742-6596/794/1/012025>

General rights

Copyright and moral rights for the publications made accessible in Discovery Research Portal are retained by the authors and/or other copyright owners and it is a condition of accessing publications that users recognise and abide by the legal requirements associated with these rights.

Take down policy

If you believe that this document breaches copyright please contact us providing details, and we will remove access to the work immediately and investigate your claim.

Spectral matching and outdoor solar to electrical conversion efficiency in thin-film silicon multi-junction solar cells

This content has been downloaded from IOPscience. Please scroll down to see the full text.

2017 J. Phys.: Conf. Ser. 794 012025

(<http://iopscience.iop.org/1742-6596/794/1/012025>)

View [the table of contents for this issue](#), or go to the [journal homepage](#) for more

Download details:

IP Address: 134.36.146.35

This content was downloaded on 14/03/2017 at 14:19

Please note that [terms and conditions apply](#).

You may also be interested in:

[Analysis of a multi-junction solar cell with shunted subcells using SPICE](#)

E D Filimonov, S A Kozhukhovskaia, M A Mintairov et al.

[Modelling of two-and four-terminal thin-film silicon tandem solar cells](#)

S Reynolds and V Smirnov

[Numerical Simulation of Silicon-on-Insulator Thin-Film Solar Cells](#)

Hideyuki Iwata, Takashi Ohzone and Hideyuki Takakura

[Fill-Factor Calculation of Solar Cells Affected by Sheet Resistance of Surface Layer](#)

Hirohiko Niu, Hideki Doi, Tetsuro Matsuda et al.

[Optimum Design of Thin-Film-Based Tandem-Type Solar Cells](#)

Hideyuki Takakura

[Field test analysis of concentrator photovoltaic system focusing on average photon energy and temperature](#)

Husyira Al Husna, Yasuyuki Ota, Takashi Minemoto et al.

[Design of periodic nano and macro scale textures for high-performance thin-film multi-junction solar cells](#)

J Krc, M Sever, M Kovacic et al.

[Microcrystalline Silicon Carbide p-Layer with Wide-Bandgap and Its Application to Single- and Triple-Junction Silicon Thin-Film Solar Cells](#)

Soohyun Kim, Jinhee Park, Hongchul Lee et al.

Spectral matching and outdoor solar to electrical conversion efficiency in thin-film silicon multi-junction solar cells

S Reynolds¹, F Urbain^{2,3} and V Smirnov²

¹ School of Science and Engineering, University of Dundee, Dundee DD1 4HN, Scotland.

² IEK-5 Photovoltaik, Forschungszentrum Jülich, D-52425 Jülich, Germany.

³ Present address: IREC Catalonia Institute for Energy Research, Barcelona, Spain.

E-mail: s.z.reynolds@dundee.ac.uk

Abstract. Semi-empirical computer modelling is used to investigate spectral matching in tandem and triple-junction thin film silicon solar cells. In amorphous/microcrystalline silicon (a-Si:H/ μ c-Si:H) tandem cells, current mis-match is offset by an increase in fill-factor, resulting in a broad peak in efficiency versus average photon energy. For a-Si:H/a-Si:H tandem cells, photo-generated currents in both sub-cells increase with increasing average photon energy, and efficiency is predicted to increase monotonically over a wide spectral range. a-Si:H/a-Si:H/ μ c-Si:H triple cells exhibit spectral behaviour similar to a-Si:H/ μ c-Si:H tandem cells, but with a smaller fill-factor dependence. Variations in spectral quality are predicted to account for only a small reduction in annual electrical energy yield, of some 2 to 4%.

1. Introduction

Stacked multi-junction solar cells enable thermalisation and transmission losses to be reduced over the constituent single-junction cells, leading to an overall increase in photovoltaic conversion efficiency. This has been utilised in the development of multi-cell combinations of thin-film (amorphous and microcrystalline) silicon, yielding laboratory efficiencies of over 14% [1-4]. Further, increased terminal voltages (> 1.5 volts) are sufficient to drive photochemical water-splitting reactions directly, an application that has attracted considerable recent interest [5-7].

Careful matching of photogenerated currents is needed to optimise efficiency for a given spectrum [1,2], which in the laboratory is normally AM1.5G. However substantial variations in the solar spectrum occur naturally; multi-junction cells seldom operate outdoors in a current-matched condition, impacting on annual energy return. We present a model [8,9] that enables these effects to be evaluated. Realistic outdoor spectra are generated using a linear weighting function, and characterised in terms of average photon energy (*APE*) [10,11]. The short-circuit currents generated by sub-cells as a function of *APE* are calculated by numerical integration, and used to scale the J-V characteristics of reference single cells from which the overall J-V characteristic is obtained. Statistical distributions of spectral irradiance vs. *APE* are used to estimate long-term outdoor performance at a given location.

2. Experimental

2.1. Solar cell deposition

All cells were deposited in p-i-n superstrate configuration by plasma-enhanced chemical vapour deposition onto TCO coated glass. The top cell absorber layer of the a-Si:H/ μ c-Si:H tandem cell was



deposited at 180 °C with a silane concentration (SC) of 10%. For the a-Si:H/a-Si:H tandem cell and the a-Si:H/a-Si:H/ μ c-Si:H triple cell, the top a-Si:H absorber layer was deposited at 130°C with a SC of 4%, and the following a-Si:H layer at 180°C with a SC of 10%. Representative measured solar cell parameters are provided in table 1. Additional details are given elsewhere [2, 7].

Single junction ‘reference’ solar cells corresponding to top, middle and bottom were deposited under the same conditions. Layers representing the top, and (top + middle) sub-cells, used to filter the solar spectrum when measuring J - V characteristics of single cells representing the middle and bottom sub-cells, were deposited on glass slides and placed in the optical path.

Table 1. Representative measured cell parameters. V_{OC} is open-circuit voltage, J_{SC} short-circuit current, FF fill-factor and η conversion efficiency.

Cell configuration	a-Si/ μ c-Si	a-Si/a-Si	a-Si/a-Si/ μ c-Si
V_{OC} (V)	1.40	1.87	2.28
J_{SC} (mA/cm ²)	11.8	6.96	8.44
FF (%)	67.4	76.3	68.0
η (%)	11.1	9.9	13.1

2.2. Solar cell characterisation

Current–voltage (J – V) measurements under standard test conditions (100 mW/cm², 25°C) were made using a double source (Class A) AM1.5 sun simulator. External quantum efficiency (EQE) measurements were conducted over the wavelength range 300 nm to 1100 nm using chopped light from a monochromator. Individual sub-cell EQEs of tandem and triple cells were determined separately, by using bias light sources to saturate those sub-cells not under measurement.

2.3 Modelling procedure

The modelling procedure has been described in detail elsewhere [8,9]. It consists of three main steps: (i) Solar spectra with APE s between 1.75 and 2.05 eV are generated by applying a linear spectral weighting function pivoted at 630 nm to the AM1.5 spectrum. The resulting spectra are similar in shape to those corresponding to a given APE [12,13]. (ii) The J_{QE} values for each sub-cell are calculated by numerical integration of the product of the EQE and a given spectrum, between 350 and 1050 nm. (iii) The relevant J_{QE} values are then used to shift each J - V curve along the current axis such that $J_{SC} = J_{QE}$. It is then straightforward to calculate points on the multi-junction J - V curve by adding the voltages for each sub-cell at the same current value.

3. Results and discussion

3.1. Sub-cell currents

The EQE data, from which J_{QE} values are computed for given model spectra, are presented in figure 1. The wavelength regimes over which each sub-cell generates photocurrent can be clearly identified. Figure 2 shows sub-cell currents vs. APE obtained when the solar spectrum is modelled for the three configurations studied here. The performance of multi-junction cells under given spectral conditions is constrained by the smallest of the currents generated by the component sub-cells. The a-Si:H/ μ c-Si:H tandem cell (figure 2(a)) is top-cell limited below $APE = 1.90$ eV, and bottom- cell limited above this. A peak in short-circuit current, of approximately 11.3 mA/cm² is predicted at around 1.90 eV. The a-Si:H/a-Si:H tandem cell (figure 2(b)) exhibits rather different behaviour. While the sub-cell currents are equal (around 7 mA/cm²) at $APE = 1.82$ eV, the short-circuit current is predicted to increase monotonically with increasing APE over the range investigated. This is a consequence of differing

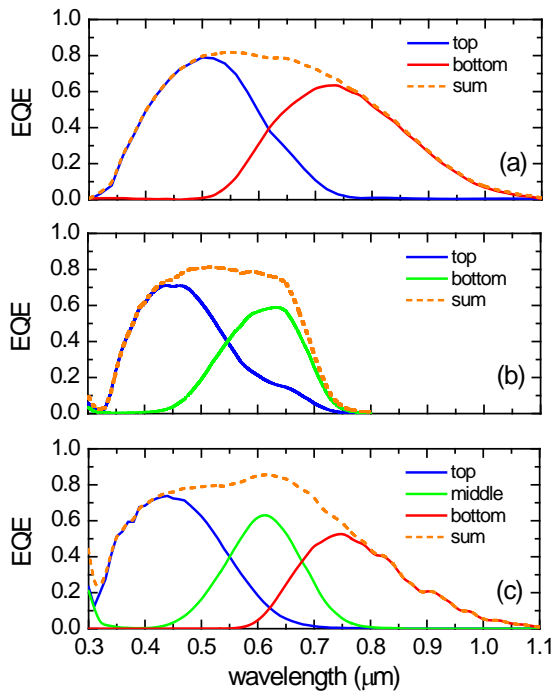


Figure 1. EQE measurements on: (a) a-Si:H/ μ c-Si:H tandem cell; (b) a-Si:H/a-Si:H tandem cell; (c) a-Si:H/a-Si:H/ μ c-Si:H triple cell.

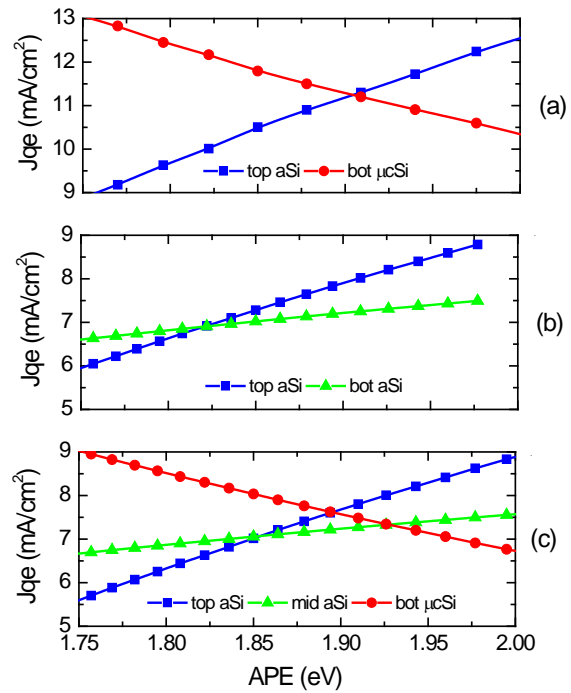


Figure 2. Modelled sub-cell currents for multi-junction cells: (a) a-Si:H/ μ c-Si:H; (b) a-Si:H/a-Si:H; (c) a-Si:H/a-Si:H/ μ c-Si:H.

band-gaps of the bottom cells in these two cases, with the former requiring a thicker top-cell to generate sufficient current to achieve optimal matching

In the a-Si:H/ μ c-Si:H tandem cell, lower-energy photons generate a substantial fraction of the μ c-Si:H bottom-cell current, as the higher-energy photons are absorbed by the thick (300 nm) top cell. This ‘shadowing’ causes the bottom-cell current to fall with increasing *APE*. In the a-Si:H/a-Si:H tandem cell however, the top cell is thinner (90 nm) and sufficient higher-energy photons are transmitted to the bottom-cell to increase the photogenerated current with increasing *APE*. As can be seen from figure 1(b), the a-Si:H bottom cell does not absorb significantly at wavelengths above 750 nm, so lower-energy photons have little bearing on performance of the a-Si:H/a-Si:H tandem. As *APE* increases beyond the range normally encountered outdoors, the a-Si:H bottom-cell current would ultimately begin to fall as the top-cell absorbs an increasing proportion of the total photon flux.

It can be seen from figure 2(c) that the a-Si:H/a-Si:H/ μ c-Si:H triple cell passes from top-cell limited to middle-cell limited (but still increasing short-circuit current) to bottom-cell limited (decreasing short-circuit current) as the *APE* is gradually increased. The triple-cell thus shares some of the properties of both tandem cells, but detailed behaviour will depend on layer thicknesses.

3.2 Fill-factor and efficiency

The variations in short-circuit current described in section 3.1 give a good indication of how the PV conversion efficiency of the tandem and triple cells will vary as a function of *APE*. However, while the open-circuit voltage does not vary greatly with *APE* [14], fill-factor may be quite strongly affected. Figure 3(a) reveals that *FF* increases significantly when the tandem cell becomes mismatched, particularly when bottom-cell limited, in agreement with [15]. This moderates the down-turn in efficiency when the short-circuit current decreases either side of the matching point. It should also be noted that the current-matched condition does not correspond exactly to the maximum-power

condition. We have previously shown [9] that maximum power is predicted to occur when the tandem cell is mis-matched by 0.8 mA/cm^2 , in favour of the top-cell. The a-Si:H/a-Si:H tandem cell (figure 3(b)) shows an increased FF when bottom-cell limited but a slight decrease when top-cell limited. Overall, efficiency increases quite strongly with increasing APE . The a-Si:H/a-Si:H/ $\mu\text{c-Si:H}$ triple-cell (figure 3(c)) simulation curves are similar to the a-Si:H/ $\mu\text{c-Si:H}$ tandem-cell, but FF variations are comparatively minor, leading to a narrower peak in efficiency. Figures 3(a) and 3(c) indicate that the power-matching for these cells occur at a bluer APE (1.93 eV) than the AM1.5G spectrum (1.88 eV).

3.3 Annual-average conversion efficiency

Figure 4 presents the PV conversion efficiencies of the three multi-junction cells as a function of APE . In order to determine whether these variations affect longer-term energy yield, a comparison between the efficiency curves and the annual-average spectral irradiance distribution must be made. This reveals variations in the position of the peak of the distribution depending on geographical location. A generic curve based on literature data has been added to figure 4 for comparison. For optimum annual energy yield, the peak in spectral irradiance distribution should be aligned with the peak in conversion efficiency. Figure 4 indicates that for the a-Si:H/ $\mu\text{c-Si:H}$ and a-Si:H/a-Si:H/ $\mu\text{c-Si:H}$ cells, the majority of the annual spectral irradiance is converted to electricity at a normalised efficiency of $>98\%$ of the peak value. More detailed calculations suggest that a 2-4% loss in annual energy due to spectral mis-match is a realistic estimate [9]. For the a-Si:H/a-Si:H cell there is no peak in efficiency, and provided the efficiency increases roughly linearly the gain at higher APE will tend to cancel the loss at lower APE . Thus spectral mis-match is predicted to have smaller impact in this case.

Figure 4 may be used to estimate the consequences of deploying cells or modules optimised for use at a specific value of APE , at a location where the most probable APE is not aligned with module peak efficiency. When the different spectral bandwidths are taken into account, distributions measured at a range of sites, including NREL (Colorado USA) [11,12], Ispra (Italy) [12], Loughborough (UK) [11]

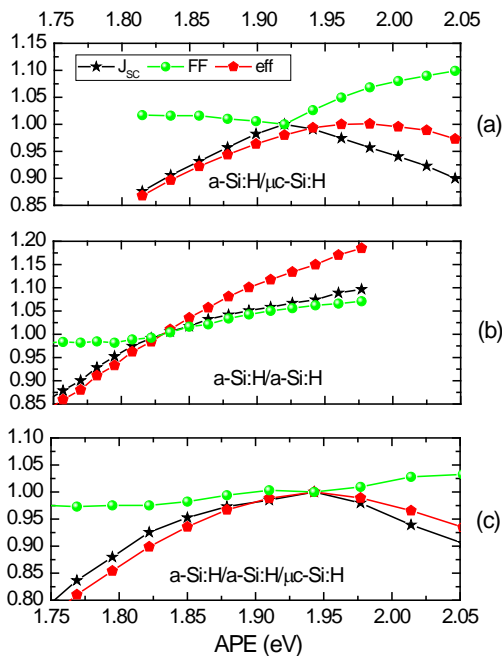


Figure 3. Modelled short-circuit current, fill-factor and efficiency for tandem and triple cells. All scales are normalised to 1.0 at the current-matched point.

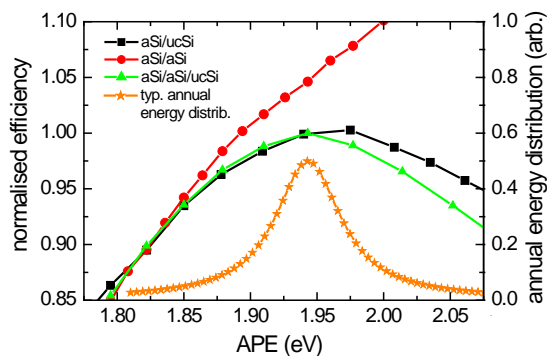


Figure 4. Modelled efficiencies for tandem and triple cells, normalised to overlap low-energy section of curves. Annual average irradiance distribution enables comparison.

and Kusatsu (Japan) [16] span a peak *APE* range of some 0.05 eV, similar to the widths of the distributions. For a tandem or triple cell matched for maximum efficiency under AM1.5G spectrum, the resulting variation in annual electrical energy production across these sites is of a similar magnitude to that due to the widths of the distributions.

Gottschalg et al [17] have differentiated band-gap effects and current mis-match effects for single and multiple cells, as ‘primary’ and ‘secondary’, respectively. Our model results indicate that the influence of these factors on long-term outdoor electrical output from multi-junction cells is complex. Spectral effects in multi-junction cells are generally minor compared with other site-related effects, such as temperature variations and degradation/annealing cycles [18], though some studies [19] suggest a greater significance.

3.4 Comparison of model predictions with laboratory and outdoor data

A number of the predictions made here, relating to variation of fill factor and the distinction between current-matching and power-matching, have been demonstrated in the lab for the case of a-Si:H/ μ c-Si:H tandem cells [14, 15, 20]. This supports the view that the approximations inherent in our model are not an over-simplification. Outdoor data are inherently quite noisy due to limitations in controlling or cancelling the influence of variables other than the set being studied, plus the non-unique nature of *APE* as a measure of spectral quality, which can make it challenging to identify trends. However, a peak in efficiency vs. *APE*, of a similar magnitude and profile to that predicted by our model, has been identified in outdoor test data from a-Si:H/ μ c-Si:H modules [16]. The tandem and triple-junction ‘amorphous silicon’ modules studied by Jardine et al [10] and Betts et al [11] behave quite similarly to our a-Si:H/ μ c-Si:H and a-Si:H/a-Si:H/ μ c-Si:H cells. Both show a peak in normalised current vs. *APE*, with that of the triple cell being more distinct, when compared with an amorphous silicon single junction. Krishnan et al [21] have performed modelling using actual spectra recorded in the Netherlands, for a-Si:H/a-SiGe:H/ μ c-Si:H triple cells. They have examined two cells, one well-matched to AM1.5G, and one poorly-matched. For the well-matched cell, the photogenerated current data agree quite well with our figure 3(c), although there are differences in detail, particularly regarding middle-cell current. This can be anticipated since the bandgap is smaller for the a-SiGe:H alloy than for our a-Si:H layer. Overall, results in the literature are in keeping with model predictions.

4. Conclusions

A semi-empirical model has been used to study the influence of solar spectral variations on current-matching in tandem and triple-junction thin film silicon solar cells, in terms of average photon energy. In a-Si:H/ μ c-Si:H tandem cells, current mis-match reduces photovoltaic conversion efficiency due to top-cell limitation at low *APE* and bottom-cell limitation at high *APE*. This is mitigated by an increase in fill-factor either side of the current-matched condition, resulting in a broad peak in efficiency vs. *APE* whose maximum occurs under slightly bottom-cell limited operation. As the majority of solar terrestrial spectral irradiance falls within a comparatively narrow *APE* range, within ± 0.04 eV of the peak cell response, spectral variation is predicted to be a minor concern, accounting for a reduction in annual electrical energy yield of some 2 to 4%.

For a-Si:H/a-Si:H tandem cells, photo-generated currents in both sub-cells increase with increasing *APE* over the range of interest. The short-circuit current thus increases monotonically, with a reduction in gradient rather than a peak being observed at the current-matched point. *FF* is not strongly influenced, with a slight increase occurring under bottom-cell limitation. A peak in efficiency with *APE* is thus not anticipated for this combination. The model predicts that a-Si:H/a-Si:H/ μ c-Si:H triple cells will exhibit spectral behaviour similar to a-Si:H/ μ c-Si:H tandem cells, but with smaller variations in fill-factor. The modelled efficiency vs. *APE* peak is slightly narrower, leading to a greater (but still small) reduction in annual electrical energy yield than for the tandem cell.

Acknowledgments

The authors are grateful to K. Wilken for preparation of certain a-Si:H/a-Si:H cells used in this work, and to F. Finger for discussions.

References

- [1] Yan B, Yue G, Sivec L, Yang J, Guha S and Jiang C 2011 *Appl. Phys. Lett.* **99** 113512
- [2] Smirnov V, Lambertz A, Tillmanns S and Finger F 2014 *Can. J. Phys.* **92** 932
- [3] Schüttauf J-W, Bugnon G, Stuckelberger M, Hänni S, Boccard M, Despeisse M, Haug F-J, Meillaud F and Ballif C 2014 *IEEE J. Photovoltaics* **4** 757
- [4] Matsui T, Maejima K, Bidiville A, Sai H, Koida T, Suezaki T, Matsumoto M, Saito K, Yoshida I and Kondo M 2015 *Jpn. J. Appl. Phys.* **54** 08KB10
- [5] Reece S Y, Hamel J A, Sung K, Jarvi T D, Esswein A J, Pijpers J J H and Nocera D G 2011 *Science* **334** 645
- [6] Urbain F, Smirnov V, Becker J-P, Rau U, Ziegler J, Kaiser B, Jaegermann W and Finger F 2015 *Sol. Energy Mater. Sol. Cells* **140** 275
- [7] Urbain F, Smirnov V, Becker J-P, Lambertz A, Yang F, Ziegler J, Kaiser B, Jaegermann W, Rau U and Finger F 2016 *Energy Environ. Sci.* **9** 145
- [8] Reynolds S and Smirnov V 2012 *J. Phys.: Conf. Ser.* **398** 012006
- [9] Reynolds S and Smirnov V 2015 *Energy Procedia* **84** 251
- [10] Jardine C N, Betts T R, Gottschalg R, Infield D G and Lane K 2002 *Proc. 'PV in Europe – From PV Technology to Energy Solutions'* (Rome, Italy)
- [11] Betts T R, Jardine C N, Gottschalg R, Infield D G and Lane K 2003 *Proc. 3rd World Conference on Photovoltaic Energy Conversion* (Osaka, Japan) p 1756
- [12] Norton M, Gracia Amillo A M and Galleano R 2015 *Solar Energy* **120** 337
- [13] Minemoto T, Nakada Y, Takahashi H and Takakura H 2009 *Solar Energy* **83** 1294
- [14] Blank B, Ulbrich C, Merdzhanova Tz., Zahren C, Pieters B E, Gerber A and Rau U 2015 *Sol. Energy Mat. Sol. Cells* **143** 1
- [15] Ulbrich C, Zahren C, Gerber A, Blank B, Merdzhanova Tz., Gordijn A and Rau U 2013 *Int. J. Photoenergy* **2013** 314097
- [16] Minemoto T, Toda M, Nagai S, Gotoh M, Nakajima A, Yamamoto K, Takatura H and Hamakawa Y 2007 *Sol. Energy Mat. Sol. Cells* **91** 120
- [17] Gottschalg R, Betts T R, Infield D G and Kearney M J 2005 *Sol. Energy Mat. Sol. Cells* **85** 415
- [18] Gottschalg R, Betts T R, Eeles A, Williams S R and Zhu J 2013 *Sol. Energy Mat. Sol. Cells* **119** 169
- [19] Virtuani A and Fanni L 2014 *Prog. Photovolt: Res. Appl.* **22** 208
- [20] Bonnet-Eymard M, Boccard M, Bugnon G, Sculati-Meillaud F, Despeisse M and Ballif C 2013 *Sol. Energy Mat. Sol. Cells* **117** 120
- [21] Krishnan P, Schüttauf J W A, van der Werf C H M, Houshyani Hassanzadeh B, van Sark W G J H M and Schropp R E I 2009 *Sol. Energy Mat. Sol. Cells* **93** 691